Dust production by abrasion of aeolian basalt sands: analogue for Martian dust

Charlie S Bristow[1] and Torsten H Moller[1]

[1] Department of Earth and Planetary Sciences, Birkbeck University of London, Malet Street, London WC1E 7HX

Corresponding author: c.bristow@ucl.ac.uk

Key Words: Mars, saltation, soil, dust, basalt, sand, particles

Key Points (up to three points in less than 140 characters)

1) Collisions between particles and surfaces during aeolian abrasion of basalt sands can produce dust.
2) Experimental results from an abrasion chamber range from less than 0.005% to 50%, by mass, of sample reduced to dust in 72 hours.
3) A Mars analogue weathered volcaniclastic sediment produced two orders of magnitude more dust than basalt dune sands.

Abstract

Dust is nearly ubiquitous on Mars, covering much of the planet's surface, having been redistributed by dust storms. Analysis of dust via landed instrumentation indicates a basaltic composition for its protolith; the same is interpreted for the dark dune sands encountered at rover field sites. In this paper, we used samples of aeolian sands derived from basaltic volcanoes in an experiment to simulate dust production from basalt dune sands within an abrasion chamber. In addition, we used samples from gypsum dunes because gypsum is found within dune fields on the northern plains of Mars. The results, expressed as weight % of sample reduced to dust, show a remarkably broad range over four orders of magnitude. Aeolian abrasion of basalt sands can produce similar amounts of dust, as is the case for some desert sands on Earth. Some plausible Mars analogue materials can produce large amounts of dust, suggesting that aeolian movement of basaltic sand, and volcanic sediments on the surface of Mars is a potential source of fine-grained sediment or dust.

Plain Language Summary

Mars is covered in dust that is stirred up and spread around the planet by dust storms. But where did the dust come from, and how was it made? We explore these questions using sands from volcanoes that were blown around in a large test tube that acts as an abrasion chamber. The results show that wind-blown particles of basalt sands and volcanic ash can produce dust. The volcanic ash produced more dust than the basalt sand, and is a likely source for some of the dust on Mars.

1. Introduction

The majority of the surface of Mars is covered by a layer of dust (Christensen, 1986), and dust plays a key role in determining the current climate on Mars (Kahn et al., 1992), and affects missions to Mars. Dust can be defined as a suspension of solid particles in a gas, or a deposit of such particles (Pye 1987). Mars dust has been described as an assemblage of clay- and fine silt-sized particles (< 5 μm), that contains primary igneous minerals: olivine, pyroxene, feldspar and magnetite, as well as sulphate-bearing alteration/weathering products (Morris et al., 2006). Berger et al. (2016) confirm a basaltic composition for Mars dust, including approximately 45-50wt% X-ray amorphous component that might be volcanic glass, with around 20wt% nanophase iron oxide. Dust is especially abundant in the regions of Tharsis, Arabia and Elysium (Christensen 1986, Bridges et al., 2010), with dust deposits reaching thicknesses of 20m or more in Arabia (Mangold et al., 2009).

The surface of Mars is cold and dry with limited chemical weathering (Cornwall et al., 2015). Given the cold and arid conditions that occur on the surface of Mars, aeolian processes dominate, including wind erosion, aeolian sediment transport and deposition (e.g. Christensen and Moore 1992, Greeley et al. 1992). These arid conditions have apparently prevailed for around 3.7 Ga (Tanaka, 1986, Ehlmann et al., 2011). On Mars there is evidence for aeolian activity from dust storms (Cantor, 2007), dust devils (Greeley et al., 2006), avalanches on dune slipfaces (Fenton, 2006, Horgan and Bell 2012a), wind ripple movement (Sullivan et al., 2008, Silvestro et al., 2010, 2013, Baker et al., 2018), sand dune migration (Silvestro et al., 2011, 2013, Bridges et al., 2012). Abrasion from saltating sand is a likely cause of erosion on the surface of Mars, and saltating sand grains could act as triggers to launch dust into suspension (Greeley et al., 1982, Bridges et al., 2012a). Greeley (2002) showed that saltating sand grains are capable of raising dust from existing dust deposits on Mars.

The origins of dust on Mars are discussed by Bridges and Muhs (2012), who suggest that most fine-grained (dust) particles on Mars are probably produced from ancient volcanic, impact, and fluvial processes. They argue that rates of primary dust production on Mars are very low and that the dust is more likely to be derived from extensive reworking of fine-grained, silt and clay sized sediments and aggregates. Greely et al. (1992) outline four potential sources for fine grained aggregates on Mars: deposits settled from the atmosphere as part of the dust cycle; ancient lake bed sediments that have since been proven to exist on Mars (Grotzinger et al., 2014, 2015); aggregates derived from evaporite crusts; and weathered surfaces disrupted by outgassing. The presence of dust as fragile, low density, sand sized aggregates that are easily entrained and transported has been confirmed by images acquired by rovers on Mars (Sullivan et al., 2008, Edgett and Newsom 2017). Such aggregates are likely to have low cohesion so that collisions that occur during saltation cause them to disaggregate (Sagan et al., 1977). In this paper we test a selection of Mars analogue sands in an abrasion chamber to determine how much dust might be produced by aeolian abrasion of basalt sands, gypsum sands, and JSC Mars 1-A Martian simulant.

On Mars, aeolian dunes are typically darker than their surrounding surfaces. The low albedo has been interpreted to indicate the presence of mafic minerals (Cutts and Smith 1973), and

a basaltic composition (Jaumann et al., 2006, Tirsch et al., 2011). In a study of low-albedo surfaces in western Arabia Terra, Edgett (2002) noted that the relations between dunes, wind streaks and subjacent areas implies that dark-toned grains, finer than those that comprise dunes, are lifted into suspension and deposited downwind. Spectral analysis of the dark dunes and sand sheets on Mars by Tirsch et al. (2011) indicates that they nearly all have the same mafic composition and that they are most likely to be derived from volcanic rocks. However, Charles et al. (2017), using thermal emission spectra, have shown that there are differences in dune sand composition. The Bagnold Dunes in Gale Crater are olivine-enriched while dunes in Ogygis Undae are olivine-deficient (Charles et al., 2017). The North polar dunes are basaltic with a hydrated mineral interpreted to be gypsum (Langevin et al., 2005, Horgan et al., 2009, Massé et al., 2012). The gypsum appears to be locally concentrated on the crests of the dunes (Calvin et al., 2009) and potentially forms around 45% of the dune sediments, although this might be a lower limit (Fishbaugh et al., 2007). Analysis of Martian soils and aeolian sands conducted by the Mars Exploration Rovers (MER) at Gusev and Meridiani show similar compositions, suggesting either global-scale mixing of basaltic material or similar regional-scale basaltic sources (Blake et al., 2013). Recent investigation of the Bagnold dunes in Gale Crater by the Mars Science Laboratory (MSL) rover Curiosity has found basaltic minerals including plagioclase, pyroxene and olivine with 42% X-ray-amorphous minerals (Achilles et al., 2017), probably volcanic glass or an alteration product such as allophane. Achilles et al. (2017) also noted remarkable similarity between the peak positions and relative intensity of the X-ray diffraction patterns at Rocknest and the Gobabeb locality on the Bagnold Dunes. Measurements at Namib and High dunes also indicate a basaltic composition for dune sands (Ehlmann et al., 2017), although Elmann et al., note that the dune sands were better sorted and contain fewer silt-sized or finer grains than other Martian soils. Ehlmann et al. (2017) also report a substantial amorphous component (35% ± 15%), that includes a sand-sized phase which is likely to be poorly crystalline hydroxylated minerals or impact or volcanic glass, as well as a second amorphous phase that is associated with finer-grained sands and soils and is possibly nanophase iron oxides.

At the Gobabeb site, on Namib dune in Gale crater on Mars, sand grains are well-rounded to sub-rounded with a high sphericity, and typically range in size from very fine to medium sand (~50 - ~500µm) (Ehlmann et al., 2017). Ripples on the nearby dune named High are composed mostly of fine to medium sand (125-500µm), and appear to be less well sorted than the sands at Gobabeb, Namib dune (Ehlmann et al., 2017). At the Rocknest sand shadow in Gale crater aeolian sediments are less well sorted and contain less than 10% coarse to very coarse particles (0.5 – 2 mm), and 40- 60% very fine to fine grained sand (100-150 µm) as well as an estimated 30 – 50% fine particles (<100 µm) (Minitti et al., 2013).

Basaltic dunes on Earth are considered to be analogues for Martian dunes (Edgett and Lancaster, 1993). But they are rare, most likely due to a combination of chemical and physical weathering on Earth's surface. While aeolian features are widespread on Mars (Cutts and Smith 1973, Greeley et al. 1992), fields of sand dunes are most common at higher latitudes with 90% of dune fields within the north and south polar regions higher than

latitude 60° (Hayward et al. 2014). This study of basaltic dune sand is relevant because the Mars Science Laboratory (MSL) 'Curiosity' rover visited the Bagnold dunes in Gale Crater (Achilles et al., 2017, Bridges et al., 2017).

In our experiment we used samples from sand dunes from Arizona, as well as the islands of Hawaii and Iceland as analogues for Martian sands. We selected these samples because the islands have a basaltic crust with little or no quartz sand and the volcanic activity is recent so that the sands have undergone only limited weathering and alteration. The likely source of the basalt sands in Arizona is dated at around 20 ka (Duffield et al., 2006), occurs in a desert environment, and shows a lack of physical and chemical weathering (Hanson et al., 2008). The selection of basalt sands for these experiments is consistent with observations of dust on Mars; for example, Goetz et al. (2005) conclude that Martian dust is formed from parent basaltic rocks by physical processes including: diurnal temperature cycles, comminution by meteoritic impacts, and wind abrasion. However, Goetz et al. (2005) also note that the dust particles cannot be exclusively unaltered 'small basaltic rocks' because the presence of ferric oxides indicates that some chemical alteration must have taken place.

Physical experiments on Mars analogue mafic minerals and basalt grains were conducted by Krinsley et al. (1979), Krinsley and Greeley (1986), Greeley et al. (1982), and Cornwall et al. (2015). Krinsley et al. (1979) constructed a Mars Erosion Devise (MED) which could operate at low pressure and simulate grain impacts under Mars atmospheric pressure. Krinsley and Greeley (1986) used the MED to simulate aeolian abrasion under Martian and Earth conditions using crushed Brazilian quartz and crushed glassy basalt from Kilauea volcano, Hawaii. Their results suggest that abrasion may be more vigorous under Martian conditions than it is on Earth due to the higher velocities required for Martian aeolian activity. They also noted the production of fine clay-sized particles, and aggregates of clay and silt-sized particles are described as ubiquitous (Krinsley and Greeley, 1986). Krinsley and Leach (1981) used an aeolian abrasion device to produce aggregates of olivine and basalt held together by electrostatic forces that were very weak and easily broken. Greeley et al. (1982) used an un-named apparatus with a rotating arm that flung sand-sized particles of quartz, basalt, basalt ash, and aggregates of fine material, at targets arranged around the inside of a chamber. They found that basalt targets were subject to similar levels of erosion when impacted by quartz grains or basalt particles. They also found that erosion rates under simulated Martian conditions are relatively high, and discuss ways in which their results might be reconciled with Mars surface geomorphology. Cornwall et al. (2015) used a modified Bond air mill to investigate the durability and rounding of mafic grains, volcanic glass and basalt rock fragments, as well as a mix of minerals, glass and basalt together. They found that olivine became rounded most rapidly and achieved a high sphericity within two hours; in contrast, augite and labradorite took slightly longer to become well rounded and retained a platy shape, never achieving a high sphericity within the two and a half hour experiments. They found that the volcanic glass and basalt were the slowest to decrease in grain size and took longer (7 hours) to become well rounded (Cornwall et al., 2015).

In this paper we investigate the production of dust particles by aeolian abrasion using Mars analogue dune sands. Aeolian sands have been selected because wind is the dominant

surface process on Mars today and in all likelihood has been the dominant process for most of Martian geologic history. The samples were collected from active sand dunes and have been subject to aeolian transport and deposition under natural physical conditions on Earth's surface. The samples include seven basaltic sand samples, three samples from Hawaii, three from Iceland and one from Arizona. In addition, we have included two aeolian gypsum sands from White Sands National Monument which are potential Mars analogue dune sands (Szynkiewicz et al., 2010), and known dust sources (Baddock et al., 2011, White et al., 2015). Furthermore, we investigated a representative split of the JSC Mars 1-A Martian regolith simulant, a volcaniclastic sediment that has not been subject to aeolian reworking. The samples are natural sediments, and with the exception of JSC Mars 1-A, they have not been sieved or processed before the experiments. The sands contain fine-grained particles, less than 63 microns, termed resident fines (Bullard et al., 2004) (Table 1).

2. Sample locations

2.1 Hawaii, USA

In this study we used samples of aeolian basaltic sand from the Ka'u desert of Hawaii (Samples DS 1, DS 2 and DS 6.2, Table 1). Sample DS 1 is a medium grained sand from the surface of a 3 m high falling dune (19^{o} 16' 36.1" N 155^{o} 22' 39.89" W). Sample DS 2 is a very coarse grained sand from a climbing dune (19^{o} 20' 39.43" N 155^{o} 18' 26.56" W). Sample DS 6.2 is a medium grained sand from a partially vegetated parabolic dune (19^{o} 21' 17.52" N 155^{o} 21' 51.59" W). For further details of these samples see Tirsch et al. (2012). Satellite images of the sample locations are included in the supplementary information. Gooding (1982) and Tirsch et al. (2012) described the petrology of basaltic sands from the Ka'u desert in Hawaii. Tirsch et al. (2012) suggest that their composition correlates very well with the composition of dark aeolian dunes on Mars. As noted by Gooding (1982) and Tirsch et al. (2012), the Ka'u desert sands are composed dominantly of glass fragments with subsidiary amounts of lithic fragments and crystals which include olivine, pyroxene, and plagioclase (Figure 1 and Table 2). However, Tirsch et al. (2012) noted that the very coarse grained sand sample DS 2 is dominated by rock fragments (Table 2), and a very coarse grained basalt clast can be seen in Figure 1B.

2.2 Iceland

Three Icelandic dune samples were used in this study; two from inland dunes near Kvensödull and one from a nebka dune close to the village of Saudarkrokur on the north coast of Iceland (65° 44' 7.61"N 19° 25' 54.58"W). The Saudarkrokur sample is very dark grey, moderately well sorted, fine-grained sand (Table 1) composed of volcanic glass and basaltic lithic particles with crystals of feldspar and olivine. The largest inland dunes in Iceland are found near Kvensödull (Arnalds et al., 2001). The dunes are dark grey and their surface is covered with wind ripples. Two surface sand samples were collected from a transverse dune that is around 500 m wide and over 10 m high (65° 53' 48.59" N 16° 21' 8.1" W). Sample KV 50 is 50 m from the upwind margin of the dune while KV 200 is a further 150 m downwind. KV 50 is very dark grey, moderately-sorted fine sand. KV 200 is very-dark grey, poorly sorted, medium-grained sand. Petrographically, the Kvensödull sands are

dominated by particles of basaltic glass, with basalt rock fragments and minor amounts of feldspar and olivine (Table 2). The medium-grained KV 200 contains more rock fragments than the fine grained KV 50 (Table 2).

2.3 Arizona, USA

The Grand Falls sample is from a falling dune on the south bank of the Little Colorado River located 500 m downstream from the Grand Falls (35° 25' 46" N 111° 12' 24" W). The dune is approximately 1 km downwind from basalt outcrops of the San Francisco volcanic field, and approximately 10 km downwind from the volcanic vents Merriam Crater and Sproul Crater. The basalt sand is likely to be derived from ash deposits of the San Francisco volcanic field (Redsteer and Hayward 2015). Duffield et al. (2006) report a near absence of physical and chemical weathering of the lavas which are believed to be around 20 ka in age (Duffield et al., 2006). The Grand Falls basalt sand is a moderately well sorted, fine-grained sand D50 162 µm (Table 1), composed of volcanic glass (80.5 %) with less than 10% basaltic rock fragments and subsidiary feldspar and olivine crystals (Table 2).

2.4 New Mexico, USA

The dune sand samples from White Sands National Monument, New Mexico, USA, are composed of gypsum and come from two different dunes. Sample T-1 is from a transverse dune close to the center of the dune field (32° 49' 14.8" N 106° 16' 37.0" W), while sample P-1 (32° 47' 41"N 106° 12' 56" W) is from a parabolic dune close to the downwind edge of the dune field. Sample T-1 is a moderately well-sorted medium-grained sand D50 289.5 µm (Table 1), while P-1 is a moderately well sorted fine-grained sand D50 272.6 µm (Table 1).

2.5 JSC Mars 1-A Martian simulant

The Johnson Space Center (JSC) Mars 1-A regolith simulant is composed of weathered volcanic ash from the Pu'u Nene cinder cone (19° 41' 47.38" N 155° 29' 51.62" W). The JSC Mars 1-A simulant has a spectral signature close to that of the dust covered regions of Mars (Allen et al. 1997, 1998), and has been used to simulate Martian dust (Calle et al. 2011), and soil (Wamelink et al., 2014). While Seifererlin et al. (2008) caution against using JSC MARS 1 for aeolian simulations due to sample variability, we find that the JSC MARS 1-A simulant is more appropriate because it has been sieved to remove particles greater than 1000 microns.**3. Methods**

3.1 Aeolian abrasion

We used an abrasion chamber based upon the designs of Whalley et al. (1982), Wright et al. (1998), Bullard et al. (2004, 2007) - modified with the addition of a second electrostatic dust trap (Figure 2)- because we found, in our tests, that dust was passing through the exhaust tube and trapping efficiency was less than previously reported. Ten grams of sample were placed in the bottom of the glass chamber and agitated by a constant stream of air with a flow rate of 28 liters per minute provided by an electric air pump. The air flow was close to the 0.0279 m^3/min^{-1} used by Bullard (2004, 2007), and sufficient to lift fine sand to elevations of around 10 cm within the test tube, although coarser sands showed less movement. The resulting impact velocities are likely to be slightly less than the impact

velocities for saltating sand. Fine particles produced by agitation and abrasion of the sample were transported vertically out of the 40 cm high abrasion chamber in suspension.

Dust produced by abrasion was collected on two electrostatic precipitators operating at 5 kV. The laboratory was climate controlled and room temperature maintained at 20° C ± 1° C and 55% ± 5% relative humidity through the experiments. At the end of each run, the brass rods and brass tubes that comprise the electrostatic dust traps were washed with distilled water to remove the dust. The water was then filtered through a pre-weighed Whatman 0.45 micron nylon membrane filter. The filters were placed in a drying oven for 24 hours and weighed again after drying. The difference in mass of the filter before and after was considered to be the mass of dust collected in the experiment. After each run, the brassware was wiped clean and dried. Gypsum is described as slightly soluble but we found that in a powdered dust form gypsum was soluble in distilled water. Due to the solubility of gypsum, we washed the brass electrostatic precipitators with acetone and then wiped them with isopropyl alcohol to remove any residue. The acetone-soaked filtrate was evaporated to dryness at room temperature and weighed as previously described. The abrasion experiments were run continuously for 72 hours for all of the samples to facilitate comparison with the results from earlier studies by Bullard et al. (2004, 2007). In addition, a second set of experiments were conducted, in which the air flow was stopped periodically, and the amount of dust collected was measured over time. In these experiments, we used representative sub-samples from Grand Falls Arizona, DS 6.2 from Hawaii, and the JSC Mars 1-A Martian simulant. The time intervals were 1, 2, 4, 8, 16 and 32 hours, extending to 119 hours for JSC Mars 1-A.

We conducted further experiments with sample JSC Mars 1-A to ensure that the dust collected was produced within the abrasion chamber. For this case we sieved the sample to isolate the coarse sand sized fraction (500-1000 microns), and the medium grain sized fraction (250-500 microns). The reason for isolating the coarse fraction,and the medium fractions, was so that we knew that the dust produced was generated within the abrasion chamber rather than mobilizing pre-existing dust sized particles, the resident fines, which were present in the original sample.

3.2 Grain size, sorting and roundness

The grain sizes of the samples were determined by dry sieving. The particle size distributions of the dust collected were measured using a Malvern Mastersizer 2000E. Portions of the nylon filters holding the dust were cut with scissors, immersed in a 50-ml vial of de-ionised water, and agitated in an ultrasonic bath for 30 seconds. The denuded filter was removed and the suspension added to a 500-ml beaker of tap water in a Malvern dispersion unit with the stirrer set at 2,000 rpm. The Malvern Mastersizer was calibrated against clean tap water and run with the Standard Operating Procedure set for 'clay'. Each sample was run five times for durations of 30 seconds. Laser obscuration values ranged between 0.14 and 7.4. Aberrant particle distribution graphs were discarded and the remaining graphs averaged for statistical grain size distribution using GRADISTAT (Blott and Pye, 2001), which

provides grain size statistics based on the graphical methods of Folk and Ward (1957). Sorting is determined as a standard deviation (ϕ) and expressed here as the inclusive graphic standard deviation (σ_1) which takes an average of the standard deviations 84-16 ϕ as well as 95 -5 ϕ (Folk and Ward 1957). Roundness can be used as an indication of the abrasion of clastic particles as shown by the sharpness of the edges and corners, independent of shape (Wadell, 1932). The roundness of particles varies within each sample and was assessed visually in comparison with standard charts portraying degrees of roundness (e.g., Pettijohn 1975).

3.3 Bulk density

Before the experiments, the bulk density of representative sub-samples was measured by pouring sand samples into a pre-weighed, graduated cylinder. The sediment mass was obtained by weighing the sediment-filled cylinder and subtracting the weight of the empty cylinder. After tapping the cylinder until no noticeable change in volume occurred, the volume of sediment was read from the graduated cylinder, and the mass of the sediment was divided by the volume to obtain a bulk density. The bulk density of the samples was measured because low density particles are more readily entrained by wind than higher density particles of a similar size.

3.4 Petrology

Representative subsamples of the sands were impregnated with epoxy resin and then cut and polished to form thin sections for petrographic analysis. In order to make a quantitative assessment of the composition of the sand grains, point-counting of 300 grains per thin section were conducted using a Swift mechanical stage. Modal analysis of petrographic thin-sections is common practice in igneous petrology (Nielson and Brockman 1977). With 300 points, the error expressed as a standard deviation is generally better than 5% (Van Der Plas and Tobi 1965), although this does not account for operator error in identifying minerals correctly. Polymineralic grains were counted as rock fragments while monomineralic grains are identified as the minerals, e.g. feldspar, or olivine. Some segregation of grains by size or density can occur during the preparation of impregnated blocks that might affect results.

3.5 Color

The color of the samples was determined by comparison with Munsell soil color charts using dry samples in daylight.

4. Results

The results of the point count analysis are shown in Table 2. Most of the basalt sands are dominated by volcanic glass. The exceptions are the two coarser grained samples DS 2 and KV 200 which contain more basaltic rock fragments. The bulk density of the basalt sands ranges from 1.42 g/cm^3 to 1.68 g/cm^3, with an average of 1.54 g/cm^3 (n = 7) (Table 1). These bulk densities are within the range of values for typical dry, desert dune sands – i.e. which range from 1.33 to 1.81 g/cm^3 with an average of 1.57 g/cm^3 (n = 1000) (Ritsema and Dekker 1994). The bulk density of the gypsum sand P1 is 1.29 g/cm^3 and T1 is 1.37 g/cm^3 (Table 1). These values are within the range of bulk densities for gypsum dune sands at

White Sands, 1.17 to 1.4 g/cm^3, with a mean of 1.3 g/cm^3 (N = 250), measured by Ritsema and Dekker, (1994). The bulk density of the JSC Mars 1-A sample is 0.87 gcm^{-3}, which is lower than the other samples (Table 1), but within the range of densities for scoria from Hawaii, 0.19 to 1.44 g/cm^3, with a mean of 0.78 g/cm^3 (n = 200) (Houghton and Wilson 1979).

The grain size of the basalt sands ranges from very coarse sand to fine sand; the sorting ranges from poorly sorted to very well sorted (Table 1). Four of the basalt sand samples are fine grained sand-sized, and moderately well sorted (DS6.2, Saudarkrokur, KV50 and Grand Falls), DS2 is very coarse sand and very well sorted. JSC Mars 1-A is fine sand-sized but poorly sorted. Two of the basalt sands are medium sand but DS1 is well sorted while KV200 is poorly sorted (Table 1). The gypsum sands are both moderately well sorted but P1 is fine sand and T1 is medium sand (Table 1).

Within the abrasion chamber the airflow was sufficient to entrain fine sand and lift it to elevations of around 10 cm within the test tube, although coarser sands showed less movement and were lifted only 1 – 2 cm. Sand particles interacted in several ways: some of the entrained particles impacted the bed and set other particles in motion, some particles collided with other grains in mid-air, some collided with the chamber walls, others rolled and occasionally avalanched at the base of the chamber, simulating a range of natural sand transporting processes and particle interactions (see supplementary video). The results of the abrasion experiments are shown in Table 3 and range from just 0.51 mg for the very-coarse grained sand DS 2, and up to 5,039 mg (JSC Mars 1-A) spanning four orders of magnitude.

Abrasion of basaltic aeolian sands from Hawaii (DS 1, DS 2 and DS 6.2) produced 4.57, 0.51 and 69.41 mg of dust, respectively. It is notable that the basalt sand sample which produced the most dust, DS 6.2, has the finer grain size (D50 = 164 µm), while the sand that produced the least dust, DS 2, has the coarsest grain size (D50 = 1148 µm). A similar scenario applies to the Icelandic samples where the range of results is not so wide (10.48 – 55.73 mg) nor is the range in grain size; however, the coarser sand (KV 200) produced the least dust (10.48 mg) and the finer grained sand (Saudarkrokur) produced the most dust (55.73 mg) (Table 3). The sample from Grand Falls Arizona, which has a D50 of 162 µm, produced a similar amount of dust (55.93 mg) as the Icelandic sample, which has a similar grain size (Table 3). The amount of dust collected over time decreases for all samples, but the amount and the rates of decrease vary between samples (Figure 5 A and B).

The grain size of the dust produced in these experiments is mainly in the silt size range with median grain size (D50) between 5.6 µm (JSC Mars 1-A), and 17.05 µm (DS2), with one exception (KV200) in which the median is 65.9 µm (Table 3). The latter is classed as very fine sand, the coarser particle size might be due to the poor sorting of KV200 and the release of resident fines.

5. Discussion

These experiments were conducted in Earth surface conditions, at room temperature and ambient air pressure. On Mars, gravity is lower and the density of the atmosphere is lower;

this results in saltating grains following a higher and longer path (Kok et al., 2012). In addition, the impact is likely to be more energetic (e.g. Greeley, 2002, Kok, 2010), with collisions resulting in increased abrasion and fracturing of grains (Krinsley et al., 1979). However, it is reasonable to expect the particles to behave in a similar manner, i.e. basalt sand particles on Mars will fracture or fragment in a similar manner to basalt sand particles on Earth. Sand fluxes on Mars are believed to be similar to those of seasonally frozen dunes in the Victoria Valley, Antarctica (Bridges et al., 2012a), which are reversing dunes (Bristow et al. 2010), and thus relatively slow moving. These experiments are not a direct simulation of aeolian abrasion under Martian conditions but use Martian analogue materials to provide some indications for the potential for dust production on Mars.

5.1 Error

The replicability of the method was tested by Bullard et al. (2004) who found that results varied by a factor of two (17.1 to 3.08 mg) after four hours. Our own repeats with sample KV50 produced values of 21.67 mg, 19.30 mg, 12.24 mg, 10.33 and 8.80 mg after 72 hours give slightly higher values but a similar range of results. As noted by Bullard et al. (2004) some of the variability can be attributed to small sample size where fracturing and fragmentation of a small number of grains will have a large impact on the total mass of dust produced. The samples used in these experiments are natural dune sands, the composition of which is inhomogeneous and thus differences in the mechanical properties of particles are expected. The electrostatic dust trap was described by Whalley et al. (1987) as having an estimated efficiency greater than 95%. Tests by Bristow and Moller (2017) showed dust in the exhaust outlet, demonstrating that dust could pass through the system. As a consequence, we added a second electrostatic dust trap to the apparatus (Figure 2). Comparing results from the two electrostatic dust traps, we have found similar amounts of dust in each trap, suggesting that the trapping efficiency might be closer to 50%. The efficiency of the electrostatic dust trap is potentially a large source of error resulting in an underestimate of the dust produced. There are other potential losses within the apparatus. Small amounts of dust adhere to the glassware and the washing of the brass electrodes is not completely effective and leaves some dust behind (Bristow and Moller 2017). The amount of dust lost in each run has not been quantified. However, it is apparent that the amount of dust recovered in each run is less than the amount of dust produced; therefore, the errors are all in the same vector and probably of a similar magnitude.

5.2 Grain size

A cross plot of dust collected against grain size for the basalt sand samples shows a negative relationship between dust production and median grain size (D50), $R^2 = 0.9299$, with coarse sands producing less dust than finer grained sands (Figure 3b). In experiments with aggregate grains, Bristow and Moller (2017) found that reducing the size of the aggregates increased the amount of dust collected, with coarse grained (500-1000 µm) aggregates producing twice as much dust as very coarse grained (1000-2000 µm) aggregates. The correlation between particle size and dust production could be a function of the number of active particles within the abrasion chamber and the resulting increase in collisions between particles. Fine-grained sands are more readily entrained, and there are a greater number of particles within a given mass of fine sand than there are within a similar mass of coarse-

grained sand. Similar plots for the fine fraction, D10, do not show such a strong relationship R^2 = 0.5815 (Figure 3a), suggesting that the concern about resident fines is less significant than the median grain size. Indeed, the relationship with the coarse fraction D90 R^2 = 0.7173, is slightly stronger than that for D10 (Figure 3c).

5.3 Armour

Within the abrasion chamber, very-coarse sand sized grains sometimes formed an armour that prevented finer grained particles from becoming entrained. The lack of entrainment results in fewer collisions between particles within the chamber, and consequently very little fracturing or fragmentation of particles, and thus very little dust is produced. Layers of very coarse grained sands overlying finer grained sands have been observed on Mars by the Mars Exploration Rovers, Opportunity (Sullivan et al., 2005) and Spirit (Sullivan et al., 2008), as well as the Mars Science Laboratory (MSL) rover Curiosity (Blake et al., 2013). Very-coarse particles have greater mass than smaller particles of the same density and require stronger airflows to be entrained. Sullivan et al. (2005) estimated local wind shear velocities of ~3 ms^{-1}, or up to 4 ms^{-1} are required to initiate motion of the coarse-grained particles depending on clast composition and density. Assuming a basaltic sand composition with a density of 3.0 g/cm^3, Blake et al. (2013) calculated a critical shear velocity of 2.6 ms^{-1}, to initiate particle motion. Sullivan et al. (2015) and Blake et al. (2013) indicate that the wind velocities required to produce the shear stress required to move coarse-grained, 1-2 mm, particles on Mars are rare. Armoured surfaces with a coarse grained lag will reduce the potential for dust production on Mars and within the abrasion apparatus. On the other hand, lower density scoria particles can be entrained at lower wind velocities than similar sized clasts of greater density.

5.4 *Resident fines*

The fine-grained particles that are present within the sand samples have been termed resident fines (Bullard et al., 2004, 2007), where fines include clay and silt sized particles less than 63 microns (Wentworth 1922). The release of these fine-grained particles will contribute to the dust produced in these experiments. We tested the hypothesis that resident fines will control dust production by cross plotting the mass of particles less than 63 µm determined by sieve analysis, against dust produced (Figure 3d and e). The plot of dust produced verses resident fines (Figure 3d) appears to show a very good correlation R^2 = 0.9897. However, plotting the results for the basalt sands alone (Figure 3e) does not show a clear relationship, correlation of R^2 = 0.022. Samples DS1 and DS 6.2 produced more dust than their resident fines, while the dust collected from DS2 is the same as the resident fines, most likely because DS2 is very coarse grained and the large grain size limited activity within the abrasion chamber. Samples from Iceland show a similar spread of results; the sample Saudarkrokur produced more dust than the resident fines content while KV50 and KV200 produced less. The cross-plot in Figure 3d is greatly influenced by the sample JSC Mars 1-A which has resident fines of 11% and produced 50% dust with a mean grain size of 5.61µm. The other samples contained fewer resident fines and produced much less dust clustering close to the origin on Figure 3D. The resulting linear trend approximates to drawing a straight line between two points, a cluster of samples with very low values and one sample

with extremely large values. The results indicate that there can be a correlation between resident fines and dust production, but this result is contingent on one sample, the Mars analogue JSC Mars 1-A. The result also demonstrates that the abrasion apparatus is creating fine particles because the amount of dust produced is more than four times the resident fines. In addition, the production of fine material can also be demonstrated by sieving JSC Mars 1-A to remove the resident fines. The sample JSC Mars 1A 250-500 µm, produced 29.7 % dust with a mean grain size of 6.83µm, having been sieved to remove resident fines. Overall, it is apparent that some dust can be released by entrainment of resident fines but it is obvious that additional dust has been produced within the abrasion apparatus.

Fine-grained particles have been observed within aeolian sand deposits on Mars. At the Rocknest sand shadow in Gale crater, aeolian sediments are estimated to contain 30 – 50 % fine particles, where fine particles are described as being smaller than 100µm, with approximately equal proportions of silt and very fine sand (Minitti et al., 2013). Mobilisation of these sediments is likely to release the resident fines.

5.5 *Roundness and sorting*

A cross plot of dust collected versus sorting shows no clear relationship (Figure 3f). The basalt sands used in these experiments are subangular to rounded (Table 1) and therefore less well rounded, and less well sorted than Martian dune sands at the Gobabeb site. The Rocknest sediment is probably more poorly sorted than the samples used in these experiments but a direct comparison is not possible due to the limited resolution of the instruments on the Curiosity rover (Minitti et al., 2013). Due to the subjective nature of particle roundness by visual estimation, and the variability of particle roundness within samples, no quantitative assessment of the relationship between roundness and dust production has been attempted here. However, other abrasion experiments (e.g. Kueppers et al., 2012) that used crushed, angular scoria show a non-linear decrease in ash (< 2 mm) produced over time that they attribute to rounding of particles. In addition, Cornwall et al., (2015) noted particle rounding in their abrasion experiments, and increased roundness is commonly associated with aeolian sediment transport (Kuenen, 1960, Garzanti et al., 2012).

5.6 Gypsum sands

The two gypsum sands from White Sands National Monument, P1 and T1, produced 199.98 mg and 51.07 mg respectively (Table 2). The sample P1, which produced more dust than T1, is finer grained. Given that the air flow is similar, it is likely that entrainment and activity of the finer sand is more vigorous; this resulted in more collisions between grains and the abrasion chamber and thus an increase in grain fracturing and fragmentation for the finer grained sand. The gypsum sand P1 produced almost twenty times as much dust as equivalent sized basalt sand (KV 200). We suggest that this can be attributed to differences in the mechanical properties of the grains. Gypsum is a relatively soft mineral with a value of 2 on Mohs hardness scale, and absolute hardness value of 3 (Mukherjee, 2012). It is also a crystal with a well-developed cleavage; this makes it fissile. As a consequence, gypsum might be more likely to fracture or fragment than the amorphous volcanic glass that is the most abundant component of the basalt sands. Our results contrast with those of

Szynkiewicz et al. (2013) who used a tumbling apparatus to simulate aeolian erosion. They found that the decrease in size of gypsum particles was less than the decrease measured for quartz particles. In addition, the quartz sand produced more dust (< 60 microns) than the gypsum. Szynkiewicz et al. (2013) suggest that the softness of the gypsum might protect the grains from significant physical erosion. However it should be noted that some of the dust sized particles from the quartz could be derived from erosion of the glass during the experiment (Szynkiewicz et al., 2013), and the quartz sand used in their experiments is MERCK analytical grade quartz which is a crushed quartz with very angular particles. Previous abrasion experiments with crushed quartz grains show that abrasion rates are higher for angular grains than rounded grains (Kuenen, 1960, Whalley et al., 1987, Wright et al., 1998, Bullard et al., 2004).

5.7 JSC Mars 1-A

The sample JSC Mars 1-A produced the most dust 5,039 mg (Table 3) which is equivalent to over 50% of the initial sample weight and four orders of magnitude greater than the very coarse grained DS 2. The difference can, in-part, be attributed to the difference in grain size; DS 2 is coarser grained and consequently was less often entrained and showed less activity than the finer grained JSC Mars 1-A. In addition, JSC Mars 1-A contains significant fines with a D10 of 43.9 microns while DS 2 has a D10 of 595.9 microns. Thus JSC Mars 1-A contains more than 10% dust sized particles (< 63 microns) at the outset which are not present in DS 2. Comparison of the results from the Iceland samples shows that grain size does make a difference. However, grain size alone cannot account for the vast difference in the results. Sieving JSC Mars 1-A to isolate the medium and coarse fractions still produced more dust than all of the other samples. Another and probably more significant difference is the composition. JSC Mars 1-A is composed of 90% glass fragments, some partially altered to palagonite, with less than 10% rock fragments. In contrast, DS 2 contains 49% rock fragments and less than 50% glass fragments and these are fresh and not altered. Furthermore, the bulk density of JSC Mars 1-A is 0.87 g/cm^3, which is less than all of the basalt sands (Table 1). The low density is in part attributed to the presence of scoria clasts which contain gas bubbles. Low density particles are more easily entrained by the wind and once entrained will be subject to collisions, fractures and fragmentation and production of dust.

5.8 Weathered glass on Mars

Low albedo sediments covering large areas of the northern lowlands of Mars are interpreted to be a poorly crystalline high silica phase interpreted to be iron-bearing volcanic glass partially obscured by a silica enriched glass rind (Horgan and Bell, 2012). Their interpretation suggests a history of explosive volcanism followed by widespread acid leaching. They suggest that glass-rich volcaniclastics are a major source of aeolian sands on Mars and that widespread surficial aqueous alteration has occurred under Amazonian climatic conditions. This combination of explosive volcanism and subsequent alteration provides a suitable scenario for the precursor to abundant dust production from weathered volcanic sands on Mars.

5.9 Comparison with desert dunes on Earth

It has been suggested that sand dunes in the Sahara are major sources of atmospheric mineral dust (Crouvi et al., 2012). The production of dust from desert dune sands has been simulated by Bullard et al. (2004, 2007), who conducted similar experiments to ours using sand samples collected from desert dunes in Australia. The average amount of dust produced by the 22 samples used by Bullard et al. (2007) is 0.61% of the initial weight. For comparison, we ran the experiments for the same duration, 72 hours, and started with the same sample weight of 10 grams. Three of the basalt sand samples (DS 6.2, Saudarkrokur, and Grand Falls), produced similar amounts of dust, 0.69%, 0.56% and 0.56% respectively (Figure 3). However, this does not adequately illustrate the difference in the range of the results. While the minimum value for the Australian sands is 0.41% and the maximum is 0.98%, the minimum value for the basalt sands expressed as a percentage is 0.005% (DS 2) and the maximum value is 50% (JSC Mars 1-A). The range of results from these experiments is much greater than the range of results from Australia. This is interpreted to be due to the range in composition of the basaltic sands, as well as the range in grain size, and bulk density. The Australian dune sands are all quartz rich (99% quartz) and mostly fine grained sands (Bullard et al., 2007). The basalt sands studied here show a wider range in grain size (Table 1), and composition (Table 2).

The apparent similarity in values between the Australian dune sands and the basalt dune sands DS 6.2, Saudarkrokur, and Grand Falls, does not necessarily indicate similar particle properties or similar modes of dust production. The most important factor affecting the amount of dust produced by aeolian abrasion of the Australian sands is the removal of clay coatings (Bullard et al., 2007). The experiments by Bullard et al. (2004, 2007) found that the rate of fine particle production was high during the first 16 hours of abrasion, and then reduced considerably after 48 hours (Bullard et al., 2004). The initial, relatively high rates of fine particle production may be attributed to the removal of resident fines (Bullard et al., 2004), that is pre-existing fine-grained particles within the sediments or weakly bonded to the surface of larger particles. While the later dust appears to contain finer particles < 10 µm, they attributed this to the removal of grain surface coatings (Bullard et al., 2004). Repeating the experiment with the basalt dune sands from Grand Falls Arizona and DS 6.2 from Hawaii shows that the dust collected from these sands does decrease slightly over time (Figure 5A). However, the Australian dune sand (R64) initially produced more dust than the basalt sands (Figure 5A) but the amount of dust collected decreased, over time, in a logarithmic manner (Figure 5A). After 64 hours of abrasion, the basalt sands from Hawaii and Arizona had produced more dust than the Australian dune sand (Figure 5A). Although the amount of dust collected after aeolian abrasion of the basalt sand from Grand Falls Arizona shows some reduction in dust production over time, the DS 6.2 rate of decline was lower (Figure 5A). The reduction in the rate of fine particle production from red desert sands was attributed to the removal of resident fines followed by removal of clay coatings (Bullard et al., 2007). There is a finite amount of grain coatings, and once removed they are unlikely to be replaced on an active dune sand, which likely contributes to gradual reduction in dust production from red desert dune sands. The basalt sands lack the red coloration and grain coatings typically associated with desert dunes (e.g. Walker 1979), and thus removal of

grain coatings can be discounted as a mechanism for producing dust. The different behavior overtime, and the more linear rate of dust production are attributed to the fracture and fragmentation of basalt sand particles. A non-linear decrease in particles < 2 mm, produced by abrasion of scoria was attributed to rounding of particles (Kueppers et al., 2012). However, their experiments used angular particles of crushed scoria whereas the particles used in our experiments were initially rounded to sub-rounded. Cornwall et al. (2015), also noted a reduction in the rate of material lost during abrasion which they attribute to the rounding of particles, as well as the fracturing of some minerals. For the JSC Mars 1A Martian simulant, the amount of dust collected decreases over time and the decrease approximates a logarithmic decay (Figure 5B). We suggest that this is due to the fracturing and fragmentation of the altered and weathered glass in JSC Mars 1-A.

5.10 Alternative models

While Bridges and Muhs (2012) acknowledge that abrasion of rocks and soil by sand blasting is capable of producing dust, they regard this as a minor process arguing that higher energy processes active on Mars in the past, such as volcanic eruptions, meteorite impacts, as well as erosion associated with channels and possibly glaciation, have been more effective dust producers. However, the surface of Mars has been dry for a very long time, potentially since the end of the Noachian around 3.7 Ga (Tanaka, 1986). This leaves a huge time span for aeolian process on the surface of Mars to produce dust, so that even if the rates of production are very low there is a vast amount of time for dust to be generated and to accumulate on an arid Martian desert. In addition, Kuenen (1960) observed that wind abrasion of quartz is 100 to 1000 times more effective over the same distance than the mechanical action of a river. Previous abrasion experiments using Martian analogue materials have shown relatively high rates of abrasion (Greeley et al., 1982, Krinsley and Greeley, 1986). In our experiments we have shown that aeolian abrasion of basalt sands can produce significant amounts of dust, and even more from one volcaniclastic sediment. This does not rule out the potential for reworking of fines. Indeed, multiple cycles of erosion are highly likely, but, given the relatively limited duration of wet conditions on Mars and the effectiveness of aeolian abrasion, these earlier cycles might also have been dry and aeolian rather than wet and fluvial. Aeolian abrasion during saltation of basalt sand, and volcaniclastics, should be considered as a potentially significant source of dust production on Mars. Volcanoes and volcanic sediments are present on Mars (Mouginis-Mark, Wilson and Zuber 1992, Wilson and Head 1994, 2007). If the volcanic particles have been physically and chemically weathered, then the potential for dust production is much greater, even though weathering of basalt on Mars differs from weathering on Earth (Hurowitz et al., 2006). Ojha et al. (2018) suggest that deflation of the Medusae Fossae Formation (MFF) is a likely source for dust on Mars based upon the chemistry of Martian dust and the MFF. While the origins of the MFF are uncertain, it was suggested that the MFF might be composed of volcanic sediments e.g. (Hynek 2003, Bradley et al. 2002, and Kerber et al 2011). Our results appear to support the hypothesis that deflation of volcanic ash could be a potent dust source on Mars.

6. Conclusions

The abrasion apparatus produces dust particles due to the agitation and abrasion of basalt and gypsum sands that are analogues for surface sediments on Mars. Some of the dust trapped can be attributed to the entrainment of resident fines, additional dust is produced within the abrasion apparatus. Our results show that aeolian abrasion of basalt sands can produce similar amounts of dust as some desert sand dunes on Earth. However, dust production from desert dune sands appears to decrease rapidly over time whilst dust production from basalt sands is maintained longer, presumably due to the fracturing and fragmentation of particles. The results suggest that fine-grained sands produce more dust than coarse grained sands within the abrasion apparatus, possibly due to greater activity and an increased number of collisions between fine grained particles. In addition, coarse sand grains can form a surface layer that prevents the entrainment of finer grained particles. Weathered volcanic glass, which might be widespread on the surface of Mars (Horgan and Bell, 2012), represented here by the Mars analogue material JSC Mars 1-A simulant, produces orders of magnitude more dust than either the basalt sands or terrestrial desert dune sands. The low bulk density of JSC Mars 1-A makes it easy to entrain and results in increased dust production through fracturing and fragmentation. Low-density scoria particles will be more easily entrained than other volcanic clasts of similar size. Saltation is known to occur on Mars (Sullivan et al. 2008, Baker et al. 2018), and is apparently widespread on the surface of Mars (Bridges et al., 2012b). Assuming that the materials used in these experiments are appropriate analogues for Martian dune sands, the results suggest that saltation of basalt sands on Mars – and weathered volcaniclastic sediments in particular – have the potential to produce significant amounts of dust.

Acknowledgements

We thank Daniela Tirsch for providing samples from the Ka'u desert in Hawaii, Joanna Nield for providing samples from Arizona and Saudarkrokur, and Anna Szynkiewicz for the gypsum sands from White Sands National Monument. The first author collected additional samples from Iceland. We would also like to thank John Cowley (UCL) for glass blowing. The manuscript has been improved by the constructive comments of the editor and three anonymous reviews, as well as a detailed and insightful review by Ken Edgett. Data used in this paper are shown in Tables 1, 2 and 3 and are archived in the Birkbeck Research Data repository (BiRD) https://doi.org/10.18743/DATA.00030. This research is not grant funded.

References

Achilles, C.N., Downs, R.T., Ming, D.W., Rampe, E.B., Morris, R.V., Trieman, A.H., et al. (2017). Mineralogy of an active eolian sediment from the Namib dune, Gale Crater, Mars. *J. Geophys. Res.* doi: 10.1002/2017JE005262.

Allen, C.C., Morris, R.V., Lindstrom, D.J., Lindstrom, M.M., & Lockwood, J.P. (1997). JSC Mars-1: Martian regolith simulant. *Lunar and Planetary Science Conference XXVIII,* Abstract number 1797.

Allen, C.C., Morris, R.V., Jager, K.M., Golden, D.C., Lindstrom, D.J., Lindstrom, M.M., & Lockwood, J.P. (1998). Martian Regolith simulant JSC Mars-1. *Lunar and Planetary Science Conference XXIX*, Abstract number 1690.

Arnalds, O., Gisladottir, F.O., & Sigurjonsson, H. (2001). Sandy deserts in Iceland: an overview. *Journal of Arid Environments* 47, 359-371.

Baddock, M.C., Gill, T.E., Bullard, J.E., Acosta, M.D., & Rivera Rivera, N.I. (2011). Geomorphology of the Chihuahuan Desert based on potential dust emissions. J. Maps, 2011, 249-259. Doi.org/10.4113/jom.2011.1178.

Baker, M., Lapotre, M. G. A., Bridges, N. T., Minitti, M. E., Newman, C. E., Sullivan, R., et al. (2018), The Bagnold dunes in southern summer: Active sediment transport on Mars observed by the Curiosity rover. *Geophysical Research Letters* doi.org/10.1029/2018GL079040.

Berger, J. A., Schmidt, M.E., Campbell, J.L., King, P.L., Flemming, R.L., Ming, D.W., et al. (2016). A global Mars dust composition refined by the Alpha-Particle X-ray Spectrometer in Gale crater. Geophysical Research Letters, 43, 67–75. https://doi.org/10.1002/2015GL066675.

Blake, D.F., Morris, R.V., Kocurek, G., Morrison, S.M., Downs, R.T., Bish, D., et al. 2013, Curiosity at Gale Crater, Mars: characterization and analysis of the Rocknest sand shadow. *Science 341*, 1239505. DOI:10.1126/Science.1239505.

Blott, S.J., & Pye, K. (2001). GRADISTAT: a grain size distribution and statistics package for the analysis of unconsolidated sediments. Earth Surface Processes and Landforms 26, 1237-1248. DOI: 10.1002/esp.261.

Bradley, B.A., Sakimoto, S.E.H., Frey, H., & Zimbelman, J.R., (2002), Medusae Fossae Formation: new perspectives from Mars global surveyor. *J. Geophysics Res.* 107, 5058. doi.10.1029/2001JE001537.

Bridges, N.T., & Muhs, D.R. (2012). Duststones on Mars: sources, transport, deposition and erosion. In Grotzinger, J.P., and Milliken, R.E., Eds. *Sedimentary Geology of Mars*, SEPM Special Publication 102, 169-182.

Bridges, N.T., Ayoub, F., Arouac, J.P., Leprince, S., Lucas, A., & Muttson, S. (2012a). Earthlike sand fluxes on Mars. *Nature 488*, p.31-34. Doi:10.1038/nature11022.

Bridges, N.T., Banks, M.E., Beyer, R.A., Chuang, F.C., Noe Dobrea, E.Z., Herkenhoff, K.E., et al. (2010). Aeolian bedforms, yardangs, and indurated surfaces in the Tharsis Montes as seen by the HiRISE camera: evidence for dust aggregates. *Icarus 205*,165-182. Doi:10.1016/j.icarus.2009.05.017.

Bridges, N.T., Bourke, M.C., Geissler, P.E., Banks, M.E., Colon, C., Diniega, S., et al. (2012b). Planet-wide sand motion on Mars. *Geology 40*, 31-34. Doi: 10.1130/G32373.1.

Bridges, N.T., Sullivan, R., Newman, C.E., Navarro, S., van Beek, J., Ewing, R.C., et al. (2017). Martian Aeolian activity at the Bagnold dunes, Gale Crater: The view from the surface and orbit. *J. Geophys. Res.*, doi: 10.1002/2017JE005263.

Bristow, C.S., Augustinus, P.C., Wallis, I.C., Jol, H.M., & Rhodes, E.J. (2010). Investigating the age and migration of reversing dunes in Antarctica using GPR and OSL, with implications for GPR on Mars. *Earth and Planetary Science Letters* 289, 30-42 doi:10.1016/j.epsl.2009.10.026

Bristow, C.S., & Moller, T.H. (2017). Testing the auto-abrasion hypothesis for dust production using diatomite dune sediments from the Bodélé Depression in Chad. *Sedimentology*. DOI: 10.1111/sed.12423.

Bullard, J.E., McTainsh, G.H., & Pudmenzky, C. (2004). Aeolian abrasion and modes of fine particle production from natural red dune sands: an experimental study. *Sedimentology 51*, p.1103-1125. Doi:10.1111/j.1365-3091.2004.00662.

Bullard, J.E., McTainsh, G.H., & Pudmenzky, C. (2007). Factors affecting the nature and rate of dust production from natural dune sands. *Sedimentology* 54, 169-182. Doi:10.111/j.1365-3091.2006.00827.

Calle, C.I., Buhler, C.R., Johansen, M.R., Hogue, M.D., & Snyder, S.J. (2011). Active dust control and mitigation technology for lunar and Martian exploration. *Acta Astronautica 69*, p.1082-1088.doi.org/10.1016/jactaastro.2011.06.010.

Calvin, W.M., Roach, L.H., Seelos, F.P., Green, R.O., Murchie, S.L., & Mustard, J.F. (2009). Compact Reconnaissance Imaging Spectrometer for Mars observations of northern Martian latitudes in summer. *J. Geophys. Res. 114*, E00D11, doi:10.1029/2009JE003348, 2009.

Cantor, B., (2007), MOC observations of the 2001 Mars planet-encircling dust storm. *Icarus 186*, 60-96. Doi:10.1016/j.icarus.2006.08.019.

Charles, H., Titus, T., Hayward, R., Edwards, C., Ahrens, C. (2017). Comparison of the mineral composition of the sediment found in two Mars dunefields: Ogygis Undae and Gale Crater – three distinct endmembers identified. *Earth and Planetary Science Letters 458*, 152-160. doi.org/10.1016/j.epsl.2016.10.022

Christensen, P.R.(1986). Regional dust properties on Mars: Physical properties, age, and history. *J. Geophys. Res. 91,* 3533-3545. doi.org/10.1029/jB09iB03p03533

Christensen, P.R., & Moore, H.J. (1992). The Martian surface layer. In Kieffer, H.H., Jokosky, B.M., Snyder, C.W., Matthews, M.S., (Eds.) *Mars*. The University of Arizona Press, 686-729.

Cornwall, C., Bandfield, J.L., Titus, T.N., Schreiber, B.C., & Montgomery, D.R.(2015). Physical abrasion of mafic minerals and basalt grains: Application to Martian aeolian deposits. *Icarus 256*, p.13-21. doi.org/10.1016/j.icarus.2015.04.020

Crouvi, O., Schepanski, K., Amit, R., Gillespie, A.R., & Enzel, Y. (2012). Multiple dust sources in the Sahara Desert: The importance of sand dunes. *Geophysical Research Letters 39*, L13401, doi:10.1029/2012GL052145, 2012.

Duffield, W., Riggs, N., Kaufman D., Fenton, C., Forman, S., McIntosh, W., et al. (2006). Multiple constraints on the age of a Pleistocene lava dam across the Little Colorado River at Grand Falls, Arizona. *GSA Bulletin 118*, 421-429. doi:10.1130/B25814.1.

Edgett, K. S. (2002). Low albedo surfaces and eolian sediment: Mars Orbiter Camera views of western Arabia Terra craters and wind streaks. Journal of Geophysical Research Planets: Planets, 107, 5038. https://doi.org/10.1029/2001JE001587.

Edgett, K.S., & Lancaster N. (1993). Volcaniclastic aeolian dunes: terrestrial examples and application to martian sands. *Journal of Arid Environments 25*, p.271-297.

Edgett, K. S., & Newsom, H.E. (2017). Dust deposited from eolian suspension on natural and spaceflight hardware surfaces in Gale crater as observed using Curiosity's Mars Hand Lens Imager (MAHLI), Paper 6017, Dust in the Atmosphere of Mars and Its Impact on Human Exploration, LPI Contribution 1966, Lunar and Planetary Institute, Houston, Texas, USA. (13–15 June 2017, Houston, Texas, USA)

Ehlmann, B.L., Edgett, K.S., Sutter, B., Achilles, C.N., Litvak, M.L., Lapotre, M.G.A. et al. (2017). Chemistry, mineralogy, and grain properties at Namib and High dunes, Bagnold dune field, Gale Crater, Mars: a synthesis of Curiosity rover observations. *J. Geophys. Res. Planets* 122, 2510-2543, doi:10.1002/2017JE005267.

Fenton, L. (2006). Dune migration and slip face advancement in the Rabe Crater dune field, Mars. *Geophysical Research Letters 33*, DOI 10.1029/2006GL027133

Fishbaugh, K.E., Poulet, F., Chevrier, V., Langevin, Y., & Bibring, J-P. (2007). On the origin of gypsum in the Mars north polar region. *J. Geophys. Res., 112*, E07002, doi:10.1029/2006JE002862, 2007.

Folk, R.L., & Ward, W.C. (1957). Brazos River bar: a study in the significance of grain size parameters. Journal of Sedimentary Petrology 27, p.3-26.

Garzanti, E., Ando, S., Vezzoli, G., Lustrino, M., Boni, M., & Vermeesch, P. (2012). Petrology of the Namib Sand Sea: Long-distance transport and compositional variability in the wind-displaced Orange Delta. Earth Science Reviews 112, p.173-189. doi:10.1016/j.earscirev.2012.02.008

Goetz, W., Bertelsen, P., Binau, C.S., Gunnlaugsson, H.P., Hviid, S.F., Kinch, K.M., et al. (2005). Indication of drier periods on Mars from the chemistry and mineralogy of atmospheric dust. *Nature 436*, p.62-65. Doi:10.1038/nature03807

Gooding, J.L. (1982). Petrology of dune sand derived from basalt on the Ka'u Desert, Hawaii. *The Journal of Geology 90*, p.97-108.

Greeley, R. (2002). Saltation impact as a means for raising dust on Mars. Planetary and Space *Science 50*, p.151-155.

Greeley, R., & Iverson, J.D. (1985). *Wind as a geological process on Earth Mars, Venus and Titan*. Cambridge Planetary Science Series 4, pp.333.

Greeley, R., Lancaster, N., Lee, S., & Thomas, P. (1992). Martian aeolian processes, sediments and features. In Kieffer, H.H., Jokosky, B.M., Snyder, C.W., Matthews, M.S., (Eds.) *Mars*. The University of Arizona Press, p.730-766.

Greeley, R., Leach, R., White, B.R., Iversen, J., & Pollack, J. (1980). Threshold windspeeds for sand on Mars: wind tunnel simulations. *Geophysical Research Letters 7*, p.121-124.

Greeley, R., Leach, R.N., Williams, S.H., White, B.R., Pollack, J.B., Krinslye, D.H., & Marshall, J.R. (1982), Rate of wind abrasion on Mars. *J. Geophys. Res. 87*, 10,009 -10,024.

Greeley, R., Whelley, P.L., Arvidson, R.E., Cabrol, N.A., Foley, D.J., Franklin, B.J., et al. (2006). Active dust devils in Gusev crater, Mars: Observations from the Mars Exploration Rover Spirit. *J. Geophys. Res. 111*, doi 10.1029/2006JE002743

Grotzinger, J. P., Sumner, D. Y., Kah, L. C., Stack, K., Gupta, S., Edgar, L., et al. (2014). A habitable fluvio-lacustrine environment at Yellowknife Bay, Gale crater, Mars. Science, 343, 1242777. https://doi.org/10.1126/science.1242777

Grotzinger, J. P., Gupta, S., Malin, M. C., Rubin, D. M., Schieber, J., Siebach, K., et al. (2015). Deposition, exhumation, and paleoclimate of an ancient lake deposit, Gale crater, Mars. Science, 350, aac7575. https://doi.org/10.1126/science.aac7575

Hanson, S.L., Duffield, W., & Plescia, J. (2008). Quaternary volcanism in the San Francisco Volcanic Field: Recent basaltic eruptions that profoundly impacted the northern Arizona landscape and disrupted the lives of nearby residents. In Duebendorfer, E.M., and Smith, E.I., eds., *Field Guide to plutons, volcanoes, faults, reefs, dinosaurs, and possible glaciation in selected areas of Arizona, California and Nevada*. Geological Society of America Field Guide 11, p.173-186, doi:10.1130/2008.fld011(08).

Hayward, R.K., Fenton, L.K., & Titus, T.N. (2014). Mars Global Digital Dune Database (MGD^3): global dune distribution and wind pattern observations. Icarus 230, 38-46.

Horgan, B.H.N, and Bell, J.F. (2012a). Seasonally active slipface avalanches in the north polar sand sea of Mars: evidence for a wind related origin. Geophysical Research Letters 39, L09201, doi:10.1029/2012GL051329,2012

Horgan, B.H.N., & Bell, J.F. (2012b). Widespread weathered glass on the surface of Mars. *Geology 40,* 391-394. Doi:10.1130/G32755.1.

Horgan, B.H.N., Bell, J.F. III., Noe Dobrea, E.Z., Cloutis, E.A., Bailey, D.T., Craig, M.A., Roach, L.H., & Mustard, J.F. (2009). Distribution of hydrated minerals in the north polar region of Mars. *J. Geophys. Res. 114*, E01005, doi:10.1029/2008JE003187, 2009.

Houghton, B.F., & Wilson, C.J.N. (1989). A vesicularity index for pyroclastic deposits. Bull. Volcanol., 51, 451-462.

Hurowitz, , J.A., McLennan, S.M., Tosca, N.J., Arvidson, R.E., Michalski, J.R., Ming, D.W., Schroder, C., & Squyres, S.W. (2006). In situ and experimental evidence for acidic weathering of rocks and soils on Mars. *J. Geophys. Res., 111*, EO2S19, doi:10.1029/2005JE002515, 2006.

Hynek, B.M. (2003). Explosive volcanism in the Tharsis region: global evidence in the Martian geologic record. *J. Geophys. Res.* 108, 1-16. Doi.org/10.1029/2003JE002062.

Jaumann, R., Stephan, K., Poulet, F., Tirsch, D., Wagner, R., Hoffmann, H., et al. (2006). Dark materials in Martian craters. *Lunar and Planetary Science. XXVII*, Abs. #1735.

Kahn, R.A., Martin, T.Z., Zurek, R.W., & Lee, S.W., (1992). The Martian dust cycle. In Kieffer, H.H., Jokosky, B.M., Snyder, C.W., Matthews, M.S., (Eds.) *Mars*. The University of Arizona Press, p.1017-1053.

Kerber, L., Head, J.W., Madeleine, J.B., Forget,F., & Wilson, L. (2011). The dispersal of pyroclasts from Apollinaris Patera, Mars: implications for the origin of the Medusae Fossae Formation. *Icarus* 216, 212-220. doi:10.1016/j.icarus.2011.07.035.

Krinsley, D., & Greeley, R. (1986). Individual particles and Martian aeolian action – A review. *Sedimentary Geology 47*, 167-189.

Krinsley, D., & Leach, R. (1981). Properties of electrostatic aggregates and their possible presence on Mars. Precambrian Research 14, 167-178.

Krinsley D., Greeley, R., & Pollack, J.B. (1979). Abrasion of windblown particles on Mars – Erosion of quartz and basaltic sand under simulated Martian conditions. *Icarus 39*, 364-384.

Kuenen, P.H. (1960). Experimental abrasion, 4. Eolian action. *Journal of Geology 70*, p.648-658.

Kueppers, U., Putz, C., Spieler, O., & Dingwall, D.B. (2012) Abrasion in pyroclastic density currents: insights from tumbling experiments. Physics and Chemistry of the Earth 45-46, 33-39. Doi:10.1016/j.pee.2011.09.002.

Langevin, Y., Poulet, F., Bibring, J-P, & Gondet, B. (2005). Sulphates in the North Polar Region of Mars detected by OMEGA/Mars Express. *Science 307*, 1584-1586. doi:10.1126/science.1109091.

Mangold, N., Ansan, V., Mason, P., Vincedon, C. (2009). Estimate of the eolian dust thickness in Arabia Terra, Mars: implications of a thick mantle (≥ 20m) for hydrogen detection. *Geomorphologie: Relief, Processus, Environment.* 23-32. Doi:10.4000/geomorphologie.7472.

Massé, M., Bourgeois, O., Le Mouélic, S., Verpoorter, C., Spiga, A., & Le Diet, L. (2012). Wide distribution and glacial origin of polar gypsum on Mars. *Earth and Planetary Science Letters 317-318*, 44-55. doi:10.1016/j.epsl.2011.11.035.

Minitti, M.E., Kah, L.C., Yingst, R.A., Edgett, K.S., Anderson, R.C., Beegle, L.W., et al. (2013). MAHLI at the Rocknest sand shadow: Science and science-enabling activities. *J. Geophys. Res. Planets* 118, 2338-2360, doi.1002/2013JE004426, 2013.

Morris, R. V., Klingelhofer, G., Schroder, C., Rodionov, D.S., Yen, A., Ming, D.W., et al. (2006). Mössbauer mineralogy of rock, soil, and dust at Meridiani Planum, Mars: Opportunity's journey across sulfate-rich outcrop, basaltic sand and dust, and hematite lag deposits, *J. Geophys. Res., 111*, E12S15, doi:10.1029/2006JE002791.

Mouginis-Mark, P.J., Wilson, L., & Zuber, M.T., (1992).The Physical Volcanology of Mars. . In Kieffer, H.H., Jokosky, B.M., Snyder, C.W., Matthews, M.S., (Eds.) *Mars*. The University of Arizona Press, 424-452.

Mukherjee, S. (2012). *Applied mineralogy applications in industry and environment*. Springer Science Business and Media 373p.

Ojha, L., Lewis, K., Karunatillake, S., & Schmidt, M., 2018, The Medusae Fossae Formation as the single largest source of dust on Mars. Nature Communications9:2867, DOI: 10.1038/s41467-018-05291-5.

Pettijohn, E.J. (1975). *Sedimentary Rocks*. Harper and Row, New York, 628p.

Pye, K. (1987). *Aeolian dust and dust deposits*. Academic Press, London, 334p.

Redsteer, M.H., & Hayward, R.K. (2015). A field comparison of basalt vs. quartz sediment transport in the Grand Falls Dune Field, northeastern Arizona, USA. Fourth International Planetary Dunes Workshop, abstract 8019, https://www.hou.usra.edu/meetings/dunes2015/pdf/8019.pdfRitsema, C.J., & Dekker, L.W. (1994). Soil moisture and dry bulk density patterns in bare dune sands. Journal of Hydrology 154, 107-131.

Sagan, C., Pieri, D., Fox, P., Arvidson, R. E., & Guinness, E. A. (1977). Particle motion on Mars inferred from the Viking lander cameras. Journal of Geophysical Research, 82, 4430–4438. https://doi.org/10.1029/JS082i028p04430.

Seiferlin, K., Ehrenfreund, P., Garry, J., Gunderson, K., Hutter, E., Kargl, G., Maturilli, A., & Merrison, J.P. (2008). Simulating Martian Regolith in the laboratory. *Planetary and Space Science 56*, 2009-2025. Doi:10.1016/j.pss.2008.09.017.

Silvestro, S., Fenton, L., Vaz, D.A., Bridges, N.T., and Ori G.G. (2010). Ripple migration and dune activity on Mars: Evidence for dynamic wind processes. *Geophysical Research Letters, 32,* DOI: 10.1029/2010GL044743

Silvestro, S., Vaz, D.A., Ewing, R.C., Rossi, A.P., Fenton, L.K., Michaels, T.I., Flahaut, J., & Geissler, P.E. (2013). Pervasive Aeolian activity along rover Curiosity's traverse in Gale Crater, Mars. Geology 41, 483-486. Doi.org/10.1130/G34162.1.

Silvestro, S., Vaz, D.A., Fenton, L.K., Geissler, P.E. (2011). Active Aeolian processes on Mars: A regional study in Arabia and Meridiani Terrae. Geophysical research Letters 38, L20201, doi: 10.1029/2011GL048955,2011

Sullivan, R., Banfield, D., Bell III, J.F., Calvin, W., Fike, D., Golombek, M., et al. (2005). Aeolian processes at the Mars Exploration Rover Meridiani Planum landing site. *Nature 436*, 58-61. Doi:10.1038/nature03641.

Sullivan, R., R. Arvidson, J. F. Bell III, R. Gellert, M. Golombek, R. Greeley, K., et al. (2008). Wind-driven particle mobility on Mars: Insights from Mars Exploration Rover observations at 'El Dorado' and surroundings at Gusev crater. Journal of Geophysical Research Planets, 113, E06S07. https://doi.org/10.1029/2008JE003101

Szynkiewicz, A., Ewing, R.C., Moore, C.H., Glamoclija, M., Bustos, D., & Pratt, L.M. (2010). Origin of terrestrial gypsum dunes – Implications for Martian gypsum-rich dunes of Olympia Undae. *Geomorphology 121*, p.69-83.doi:10.1016/j.geomorph.2009.02.017

Szynkiewicz, A., Modelska, M., Buczynski, S., Borrock, D.M., & Merrison, J.P. (2013) The polar sulfur cycle in the Werenskioldbreen, Spitsbergen: Possible implications for understanding the deposition of sulphate minerals in the North Polar Region of Mars. *Geochimica et Cosmochimica Acta 106*, 326-343. Doi.org/10.1016/j.gca.2012.12.041.

Tanaka, K.L. (1986). The stratigraphy of Mars. *Journal of Geophysical Research 91* (B13):E139-58

Tirsch, D., R. Jaumann, A. Pacifici, & Poulet, F. (2011). Dark aeolian sediments in Martian craters: Composition and sources, *J. Geophys. Res.,* 116, E03002, doi:10.1029/2009JE003562.

Tirsch, D. (2012). Spectral and petrologic analyses of basaltic sands in Ka'u Desert (Hawaii) – implications for the dark dunes on Mars, *Earth Surf. Process. Landforms 37*, 434–448. Doi:10.1002/esp.2266.

Wadell, H. (1932). Volume, shape and roundness of rock particles. Journal of Geology 40, 1367-1368.

Walker, T.R. (1979). Red colour in eolian sands. In: Mc Kee, E.D. (Ed.) *A Study of Global Sand Seas. USGS Prof. Pap. 1052*, 62-81.

Wamelink, G.W.W., Frissel, J.Y., Krijnen, W.H.J., Verwoert, M.R., Goedhart, P.W. (2014). Can plants grow on Mars and the Moon: A growth experiment on Mars and Moon soil simulants. *PLoS ONE 9*(8): e103138. Doi.org/10.1371/journal.pone.0103138

Wentworth, C.K. (1922). A scale of grade and class terms for clastic sediments. Journal of Geology 30, p.377-392.

Whalley, W.B., Marshall, J.R., & Smith, B.J. (1982). Origin of desert loess from some experimental observations. *Nature 300*, 433-435.

Whalley, W.B., Smith, B.J., McAlister, J.J., & Edwards, A.J. (1987). Aeolian abrasion of quartz particles and the production of silt-size fragments: preliminary results. In Frostick, L., and Read, I., (Eds.), *Desert Sediments: Ancient and Modern*. Geological Society Special Publication 35, 129-138.

White, W. H., Hyslop, N. P., Trzelpa, K., Yatkin, S., Rarig, R. S. Jr., Gill, T. E., & Jin, L. (2015). Regional transport of a chemically distinctive dust: Gypsum from White Sands, New Mexico (USA). Aeolian Research, 16, 1–10. https://doi.org/10.1016/j.aeolia.2014.10.001

Wilson, L., and Head J.W. (1994). Mars: Review and analysis of volcanic eruption theory and relationship to observed landforms. Review of Geophysics 32, 221-263. doi.org/10.1029/94RG0113.

Wilson, L., & Head, J.W. (2007). Explosive volcanic eruptions on Mars: tephra and accretionary lapilli formation, dispersal and recognition in the geologic record. *J. Volcanol. Geotherm. Res.* 163, 83-97. Doi:10.1016/j.volgeores.2007.03.007.

Wright, J., Smith, B.J., & Whalley, W.B. (1998). Mechanisms of loess-sized quartz silt production and their relative effectiveness: laboratory simulations. *Geomorphology 23*, 15-34.

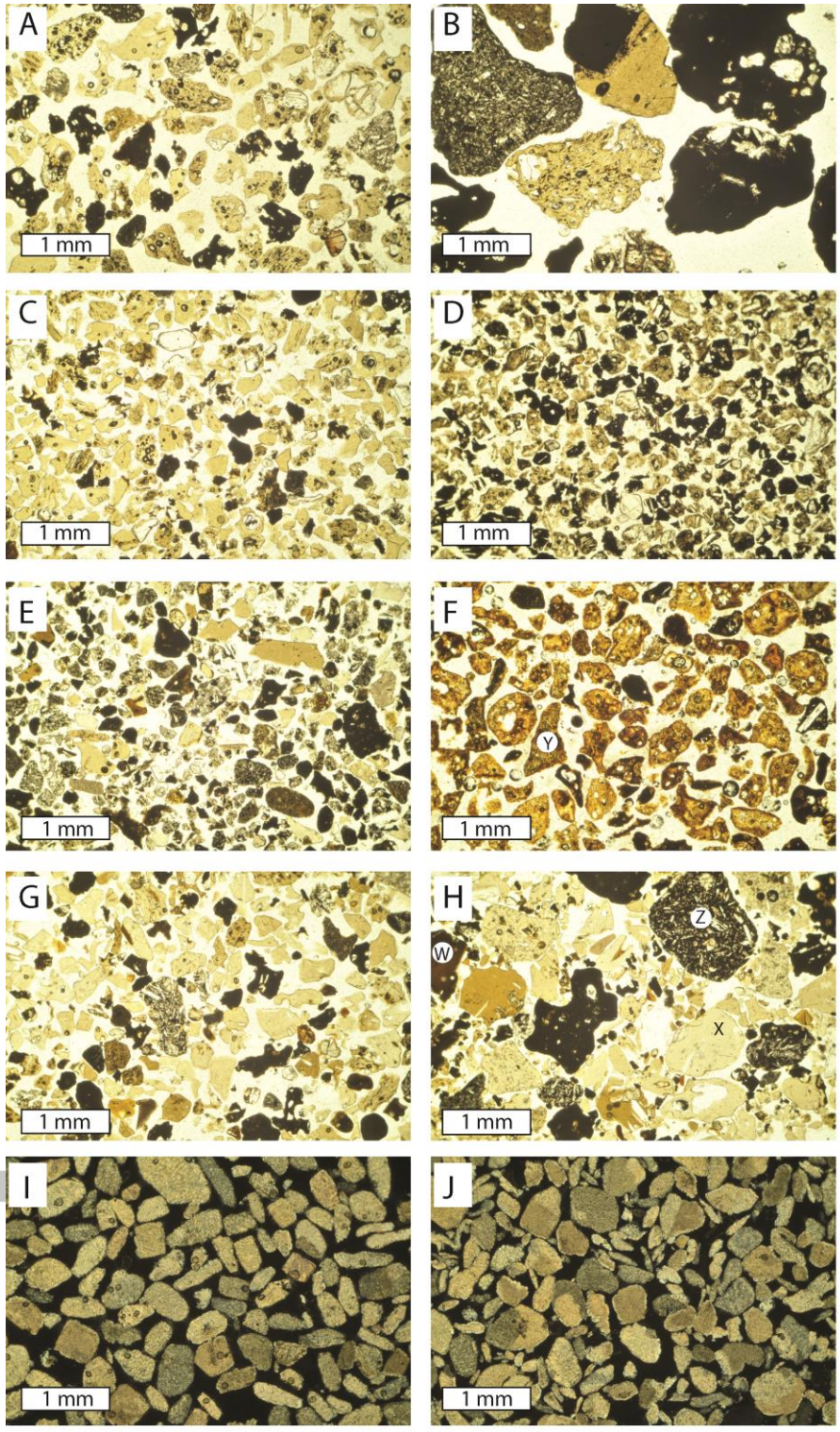

Figure 1. Photomicrographs of petrographic thin sections prepared from unconsolidated sands mounted in epoxy resin. The field of view for each photomicrograph is 4.4 mm. Photographs A to H were taken in plain polarized light. Photographs I and J were taken with crossed polars because gypsum is clear and almost translucent in plain polarized light. Descriptions of each sample can be found in the text: A) DS1, Hawaii, USA. B) DS2, Hawaii, USA. C) DS6.2, Hawaii, USA. D) Grand Falls, Arizona, USA. E) Saudarkrokur, Iceland. F) JSC Mars 1-A 250-500 µm, Hawaii, USA. G) KV50, Kvensödull, Iceland. H) KV200, Kvensödull,

Iceland. I) P1, gypsum, New Mexico, USA. J) T1, gypsum, New Mexico, USA. The letters W, X, Y and Z respectively, show examples of dark glass, fresh glass, altered glass, and a basalt rock fragment.

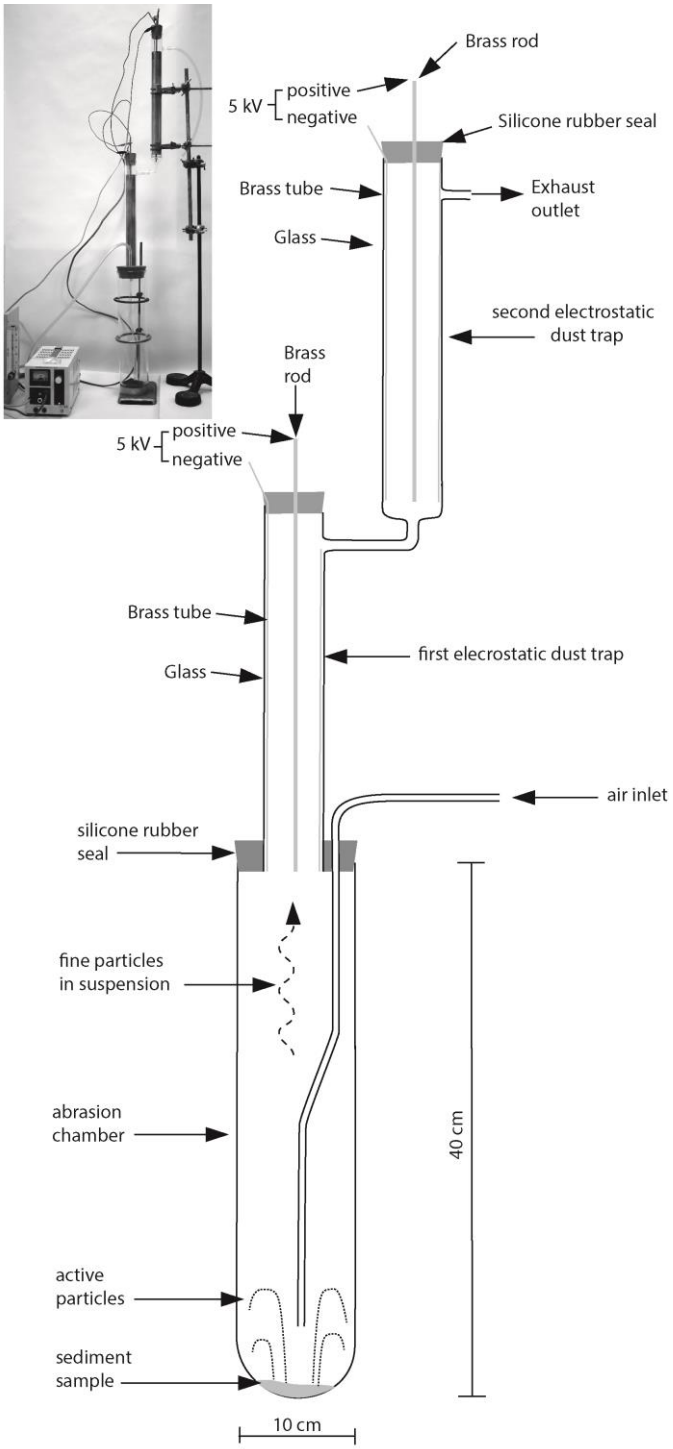

Figure 2. Schematic diagram of the abrasion apparatus used for the experiments with inset photograph.

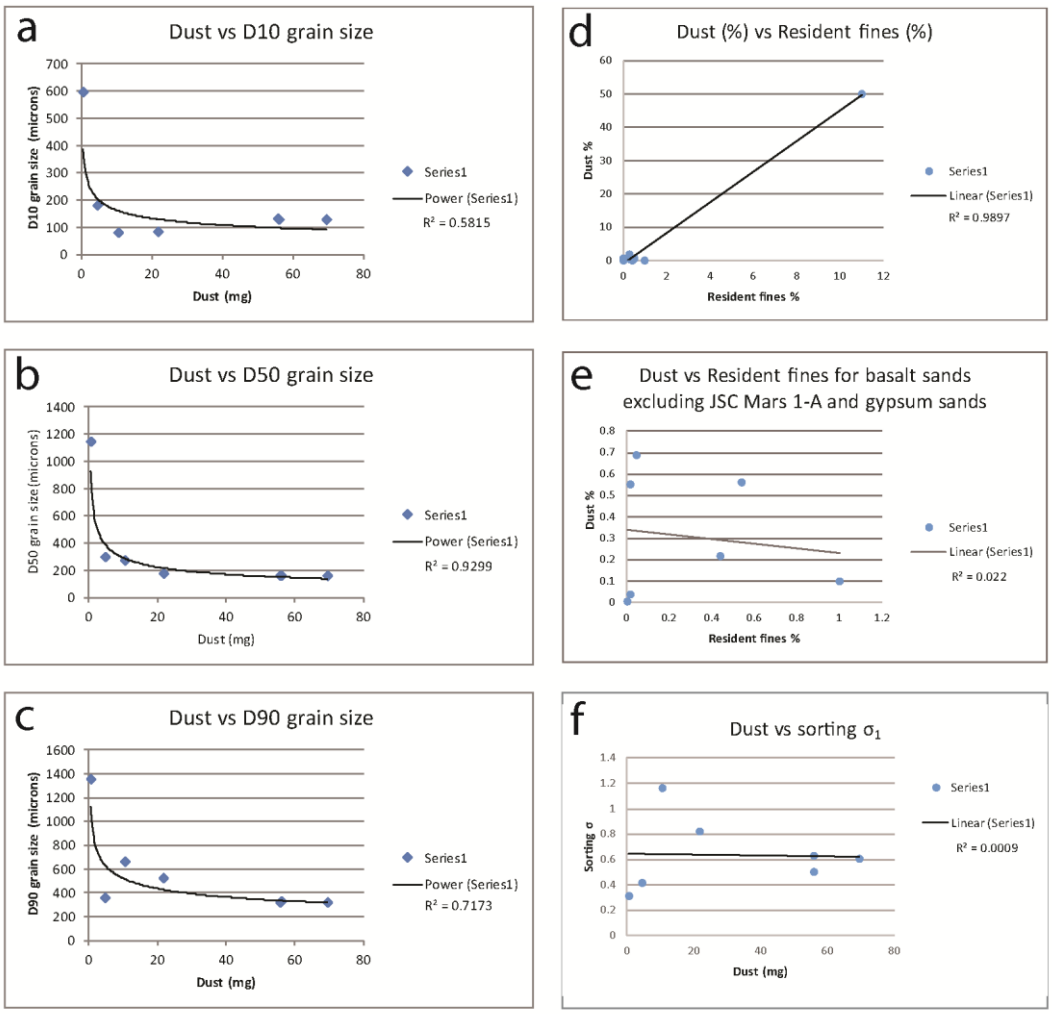

Figure 3. Cross-plots of dust collected after aeolian abrasion of basalt sands for 72 hours: (a) dust against D 10, (b) median grain size (D 50), (c) the coarse fraction D90, (d) dust mass and resident fines including JSC Mars 1-A, (e) dust mass against basalt sands without JSC Mars 1-A and the gypsum sands, (e) dust vs sorting.

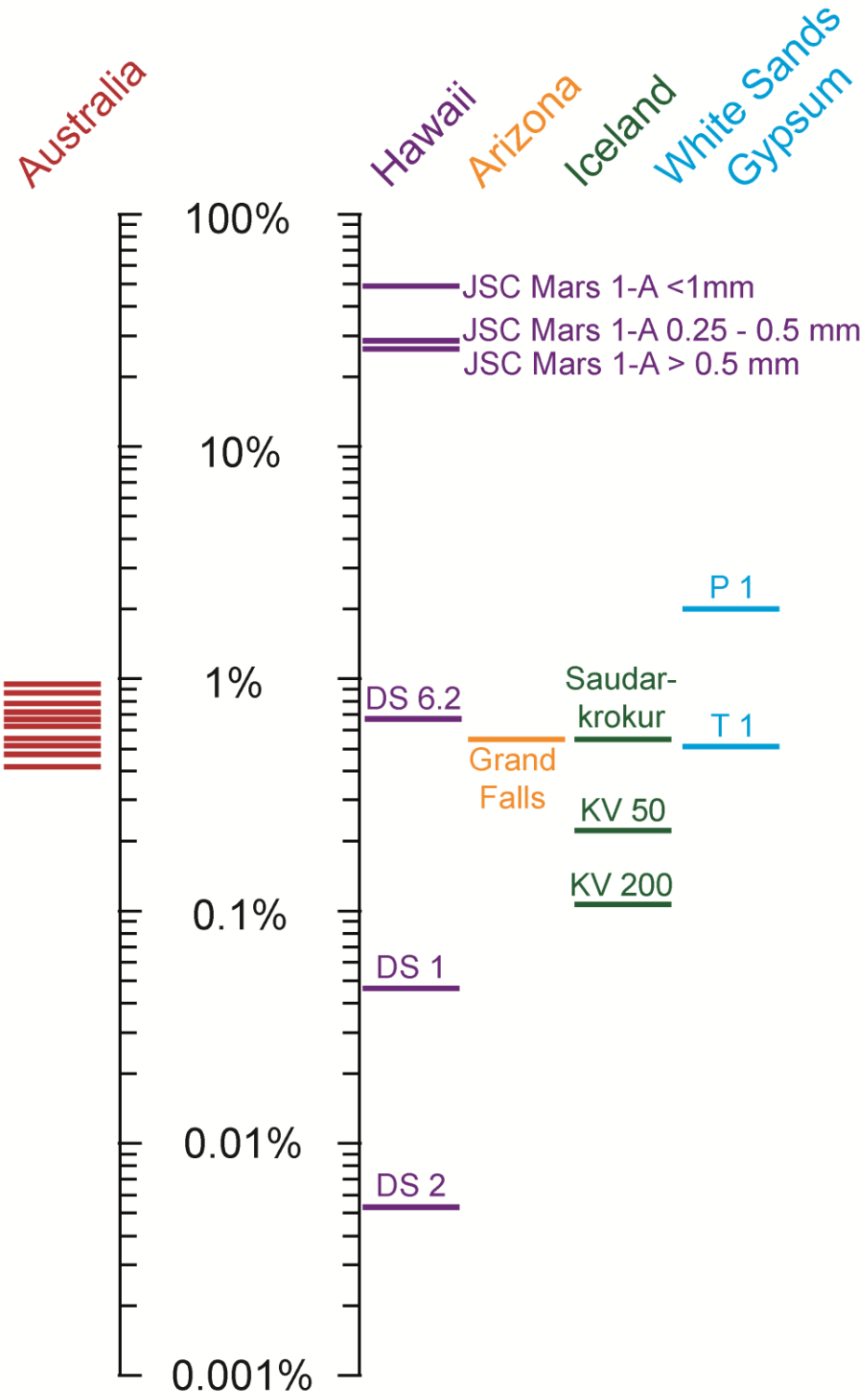

Figure 4. Distribution of dust collected after 72 hours of aeolian abrasion of basaltic sands shown as a percentage of the initial sample weight. The vertical axis has a logarithmic scale to encompass the four orders of magnitude difference in results. On the left side are results of aeolian abrasion of red-colored desert dune sands from Australia, from Bullard et al., (2007).

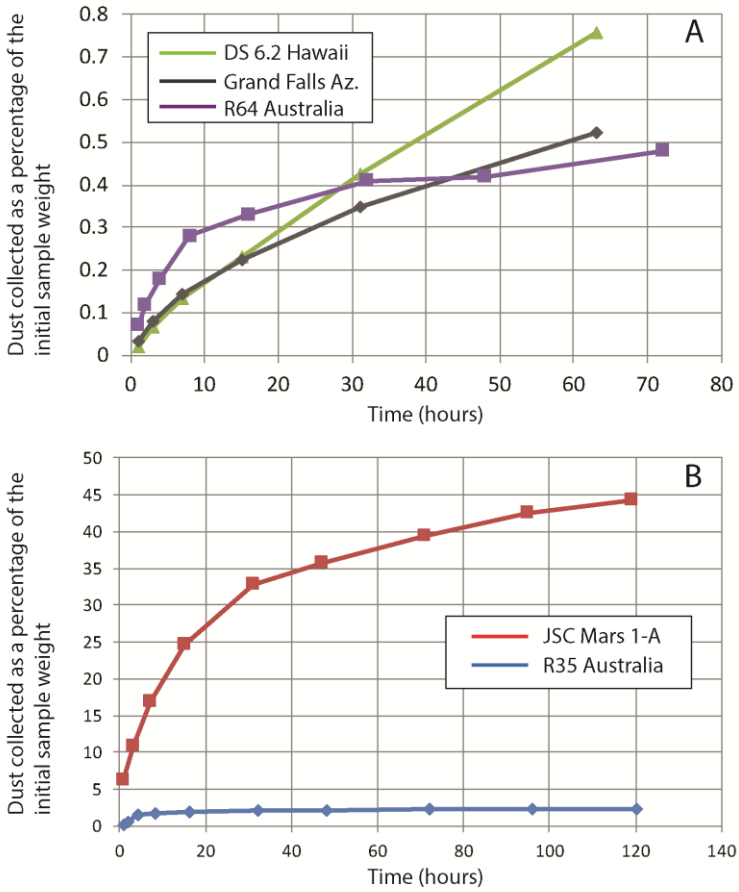

Figure 5A. The amount of dust collected after aeolian abrasion of basaltic dune sands from Grand Falls Arizona, and DS 6.2 from Hawaii, compared with a red-colored, quartz-rich dune sand from Australia R64 from Bullard et al., (2004). B. The amount of dust collected after aeolian abrasion of JSC Mars 1-A Martian simulant over 119 hours compared with a quartz rich dune sand from Australia from Bullard et al., (2004). Note the difference in the vertical axes with results expressed as weight percent of the initial sample mass.

Table 1. Sample locations, grain size characteristics, bulk density and color.

Sample name	Location State/ Country	Latitude N	Longitude W	Grain size	D 10 (µm)	D 50 (µm)	D 90 (µm)	Resident fines % (< 63 µm)	Sorting (σ_1)	Roundness	Bulk density (gcm^{-3})	Color
DS1	Hawaii USA	19° 16' 36"	155° 22' 40"	Medium sand	179	298	354	0.02	well sorted 0.417	subrounded	1.42	Hue 5Y black 2.5/1
DS2	Hawaii USA	19° 20' 42"	155° 18' 23"	Very coarse sand	596	1148	1350	0.005	very well sorted 0.315	subangular	1.63	Hue 5Y very dark grey 3/1
DS6.2	Hawaii USA	19° 21' 16"	155° 21' 50"	Fine sand	128	164	321	0.05	moderately well sorted 0.606	subangular	1.46	Hue 5Y black 2.5/1
Saudark rokur	Iceland	65° 44' 7.6"	19° 25' 55"	Fine sand	131	163	323	0.02	moderately well sorted 0.506	subrounded	1.58	Hue 5Y very dark grey 3/1
KV50	Iceland	65° 53' 31"	16° 19' 21"	Fine sand	79	178	667	0.44	moderately well sorted 0.818	subrounded	1.58	Hue 5Y very dark grey 3/1
KV200	Iceland	65° 53' 34"	16° 19' 16"	Medium sand	83	274	524	1.0	poorly sorted 1.164	rounded	1.68	Hue 5Y very dark grey 3/1
Grand Falls	Arizona USA	35° 25' 46"	111° 12' 24"	Fine sand	127	162	330	0.54	moderately well sorted 0.631	rounded	1.44	Hue 2.5 black N2.5
JSC Mars 1-A	Hawaii USA	19° 41' 45"	155° 29' 46"	Fine sand	44	166	567	11	poorly sorted 1.192	rounded	0.87	Hue 10Yr dark yellowish brown 3/4
P-1	New Mexico USA	32° 47' 41"	106° 12' 56"	Fine sand	134	273	339	0.27	moderately well sorted 0.521	rounded to well rounded	1.29	Hue 10Yr white 8/2
T-1	New Mexico USA	32° 49' 15"	106° 16' 37"	Medium sand	145	290	349	0.32	moderately well sorted 0.565	rounded	1.37	Hue 10Yr white 8/1

Table 2. Petrology of the basaltic sands

Sample name	Fresh glass	Dark Glass	Altered Glass	Total Glass	Lithic rock fragments	Feldspar	Olivine	Others
DS1	61.3	9.3	15.0	85.6	9.0	0.6	1.6	3.0
DS2	8.3	4.3	35.0	47.6	48.6	0.6	2.0	1.0
DS6.2	73.3	8.0	10.3	91.6	1.0	1.0	5.6	0.6
Saudarkrokur	19.0	9.6	18.6	47.2	39.6	4.6	2.6	5.6
KV50	51.3	23.6	14.3	89.2	8.0	1.6	0.6	0.3
KV200	45	11.3	16.3	72.6	19	6	1.6	0.6
Grand Falls	22.6	20.3	37.6	80.5	9.6	5.0	4.0	0.6
JSC Mars 1A < 1mm	0	74.9	16.3	91.2	8.6	0	0	0

Table 3 Results of the aeolian abrasion experiments. The amount of dust collected in milligrams (mg), and grain size in microns (µm).

Sample name	**Location**	**Dust** (mg)	**Dust** (%)	**First trap (lower)**				**Second trap (higher)**			
				Mean grain size of dust (µm)	**D 10** (µm)	**D50** (µm)	**D 90** (µm)	**Mean grain size of dust** (µm)	**D 10** (µm)	**D 50** (µm)	**D 90** (µm)
DS1	Hawaii, USA	4.57	0.04	10.27	1.8	7.99	115.1	15.9	2.42	13.0	117.7
DS2	Hawaii, USA	0.51	0.005	16.00	2.86	11.9	113.4	17.05	2.75	16.5	99.6
DS6.2	Hawaii, USA	69.41	0.69	11.42	2.28	12.3	46.1	8.51	2.09	7.74	88.1
Saudarkrokur	Iceland	55.73	0.55	9.12	1.73	9.69	39.9	7.93	1.84	7.97	32.9
KV50	Iceland	21.67	0.21	11.28	2.12	12.0	50.7	10.28	1.93	8.07	149.5
KV200	Iceland	10.48	0.10	65.93	3.88	49.5	976.1	17.48	2.25	23.2	95.1
Grand Falls	Arizona, USA	55.93	0.56	6.94	1.46	6.37	38.5	6.57	1.53	6.05	36.3
JSC Mars 1A < 1mm	Hawaii, USA	5,039	50.3	9.2	2.42	10.0	27.6	5.61	1.79	5.89	14.9
JSC Mars 1A 250-500 µm	Hawaii, USA	2,967	29.7	7.34	1.99	7.88	22.1	6.83	1.99	7.16	20.1
JSC Mars 1A >500 µm	Hawaii, USA	2,526	25.3	6.51	1.81	7.05	18.5	10.9	2.77	11.9	32.7
P1 (gypsum)	New Mexico, USA	199.9	1.99	na	na	na	na	na	na	na	na
T1 (gypsum)	New Mexico, USA	51.07	0.51	na	na	na	na	na	na	na	na